

Geophysical Research Letters

RESEARCH LETTER

10.1029/2019GL083642

Key Points:

- Interactions among cloud albedo, sea surface temperature, and atmospheric circulation are studied
- Cloud-ocean-atmosphere interactions act to homogenize the net cloud radiative effect over the tropical warm pools
- Shading of the ocean by convective clouds reduces sea surface temperature gradients and the degree of large-scale convective aggregation

Supporting Information:

- Supporting Information S1

Correspondence to:

C. J. Wall,
cawall@ucsd.edu

Citation:

Wall, C. J., Hartmann, D. L., & Norris, J. R. (2019). Is the net cloud radiative effect constrained to be uniform over the tropical warm pools?. *Geophysical Research Letters*, *46*, 12,495–12,503
<https://doi.org/10.1029/2019GL083642>

Received 8 MAY 2019

Accepted 23 SEP 2019

Accepted article online 15 OCT 2019

Published online 3 NOV 2019

Is the Net Cloud Radiative Effect Constrained to be Uniform Over the Tropical Warm Pools?

Casey J. Wall^{1,2} , Dennis L. Hartmann² , and Joel R. Norris¹ 

¹Scripps Institution of Oceanography, University of California, San Diego, La Jolla, CA, USA, ²Department of Atmospheric Sciences, University of Washington, Seattle, WA, USA

Abstract Global radiative-convective equilibrium simulations are used to investigate the hypothesis that mutual interactions among cloud albedo, sea surface temperature gradients, and atmospheric circulation constrain the net cloud radiative effect (CRE) to be similar in convective and nonconvective regions over the tropical warm pools. We perform an experiment in which convective clouds interact naturally with the ocean and atmosphere by forming over the warmest water and shading it and an experiment in which this interaction is removed by randomizing cloud shading of the ocean. Removing the cloud shading interaction enhances sea surface temperature gradients, lateral atmospheric heat transport, and large-scale convective aggregation and produces convective clouds with much more negative net CRE. These findings support the hypothesis that feedbacks between sea surface temperature and convection are critical to obtaining similar net CRE in convective and nonconvective regions over the tropical warm pools.

Plain Language Summary Convective clouds that form over the tropical oceans have a high albedo and a strong greenhouse effect. These radiative effects partially cancel, however, and as a result the net effect of clouds on the top-of-atmosphere radiation balance is about the same in convective and adjacent nonconvective regions. Why this happens is unknown, but one hypothesis predicts that the shading effect of convective clouds on the underlying ocean constrains the radiative properties of convective clouds and maintains a similar radiation balance in convective and nonconvective regions. We investigate this hypothesis using idealized climate model simulations. In simulations where convective clouds are able to seek out the warm parts of the ocean and shade them from incoming solar radiation, the clouds have similar net radiative effects in convective and nonconvective regions. But in simulations where convective clouds are prevented from systematically shading the warm parts of the ocean, the convective clouds become brighter and the radiative contrast between convective and nonconvective regions is enhanced. The results support the hypothesis that the interaction between sea surface temperature and shading of the ocean by convective clouds is a key mechanism for producing a similar radiation balance in convective and nonconvective regions of the tropics.

1. Introduction

Deep convection is fundamental to tropical climate. It produces extended canopies of ice clouds that regulate the absorption of solar radiation by Earth and the emission of terrestrial radiation to space. The impact of clouds on the radiation budget can be measured by the cloud radiative effect (CRE), which is defined as the difference between the top-of-atmosphere radiative flux that is observed and the flux that would be observed if clouds were removed leaving all else unchanged. Observationally based estimates of CRE, which are shown in Figure 1, indicate that the average shortwave (SW) and longwave (LW) CRE reach values up to ± 60 – 80 W/m² over the warm pools of the tropical western Pacific and Indian Oceans, where convection is common. Deep convective clouds therefore strongly influence the SW and LW components of the tropical radiation budget.

One intriguing feature that can be seen in Figure 1 is that the average SW CRE and LW CRE are individually large but nearly cancel over the warm pools. The cancellation is so close, in fact, that the distinction between convective and nonconvective regions, which is clearly seen in the SW CRE and LW CRE, is barely discernable in the net CRE. More intriguing still is the diversity of cloud types that combine to achieve this cancellation. Individual convective systems contain thick clouds with large negative net CRE and thinner extended anvil clouds with positive net CRE, yet the proportion of thick and thin clouds is such that their aggregate net

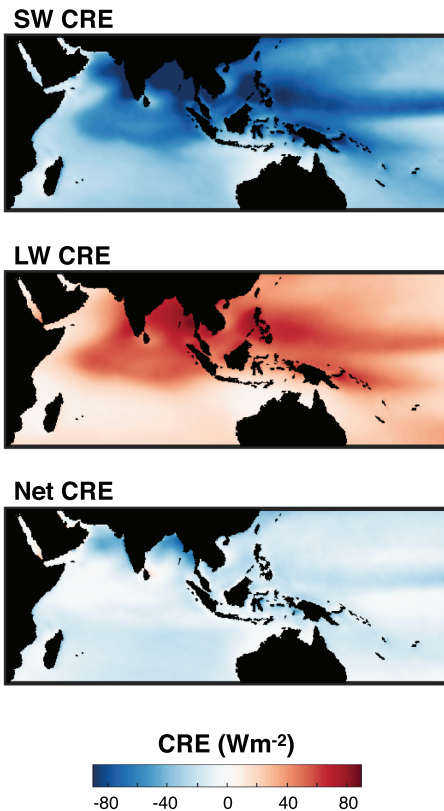


Figure 1. Climatology of CRE over the tropical warm pools. The averages are computed from Clouds and the Earth’s Radiant Energy System satellite measurements from June–August of 2000–2015. CRE = cloud radiative effect; LW = longwave; SW = shortwave.

CRE is very close to that in nonconvective regions nearby (Gasparini et al., 2019; Hartmann et al., 2001; Hartmann & Berry, 2017; Li et al., 2019; Wall et al., 2018; Wall & Hartmann, 2018).

It is currently unknown if the homogeneity of net CRE over the warm pools is coincidental or is maintained by a feedback process, but the explanation could have importance for tropical climate. For instance, the degree to which net CRE remains homogeneous in the future has significant implications for climate sensitivity. The homogeneity of net CRE is also relevant for many theories of tropical climate because conceptual models of the tropics are often based on the assumption that deep convective clouds are radiatively neutral (e.g., Clement & Seager, 1999; Miller, 1997; Peters & Bretherton, 2005; Pierrehumbert, 1995). Whether these theories are valid for past or future climates depends on whether homogeneous and near-zero net CRE is a climate-invariant feature of convective regions in the tropics. These are ample reasons to seek an explanation for why the net CRE is nearly homogeneous over the warm pools.

One possible explanation for the homogeneity of net CRE, which was proposed by Hartmann et al. (2001), is that cloud shading of the ocean dampens inhomogeneities in the top-of-atmosphere radiation balance. Convection preferentially develops over the warmest sea surface temperatures (SSTs), so cloud shading cools the warmest SST and therefore maintains small SST gradients within the warm pool. It is posited that small SST gradients reduce the efficiency of lateral energy transport by the atmospheric circulation within the warm pool region. A sufficient reduction in lateral atmospheric energy transport is expected to drive the radiation balance in convective regions toward that in nearby nonconvective regions to close the energy budget. Thus, the net CRE must be similar in convective and nonconvective regions of the warm pools. The goal of this study is to test this hypothesis using an idealized climate model.

2. Review of Hypothesis

Hartmann et al. (2001) proposed a conceptual model of the tropical warm pools. In their model, which is illustrated in Figure S1 in the supporting information, the warm pool is represented by a region of large-scale ascent and active convection and a region of subsidence and suppressed convection. The two regions are connected by an overturning cell with a horizontal scale of around 1,500 km, which is larger than individual convective systems but small enough that it is entirely contained within the warm pool region. The energy budget of the model is a balance between heat storage, net radiative input, and lateral energy transport:

$$c \frac{dT_c}{dt} = R_c - \frac{M}{A_c} c_p \Delta \theta_e - X,$$

$$c \frac{dT_n}{dt} = R_n + \frac{M}{A_n} c_p \Delta \theta_e - X.$$

In these equations the subscripts “c” and “n” indicate the convective and nonconvective regions, respectively. The left side represents heat storage by the ocean and atmosphere, the variable T is SST, and c is the heat capacity of the ocean mixed layer and atmosphere. On the right side, the term R is the top-of-atmosphere net radiation. The middle term on the right side represents heat transported between the two regions by the overturning cell. It is assumed that convection efficiently mixes heat vertically and that weak horizontal temperature gradients occur in the free troposphere. The lateral heat transport by the overturning cell is then proportional to the mass flux of the cell, M , and to the SST contrast between the two regions. The variable c_p is the specific heat capacity of air, θ_e is the equivalent potential temperature of air in contact with the surface, $\Delta \theta_e$ is the difference in θ_e between the two regions, and A is the area of the convective or nonconvective region. The final term on the right side, X , represents energy exported from the warm pool to

other regions of the planet by the atmosphere and ocean. The model assumes that, to first order, the radiative effects of convective clouds can be understood in terms of their interaction with nearby regions in the tropics, while remote interactions with the extratropics are represented by a constant heat sink.

Two additional parameterizations are made regarding clouds and circulation. First, it is assumed that albedo in the convective region increases in proportion to the strength of upward motion, which agrees with observations (Wall & Hartmann, 2018). Second, it is assumed that the strength of the overturning cell increases in proportion to the SST gradient. This assumption is supported by the fact that low-level winds in the tropics are well predicted by pressure gradients caused by SST gradients, suggesting that SST gradients have a significant influence on tropical circulations (Back & Bretherton, 2009; Li & Carbone, 2012; Lindzen & Nigam, 1987). In reality, however, many additional factors such as water vapor, LW radiation, surface heat fluxes, and convection all interact with the large-scale circulation independently of SST gradients (e.g. Becker et al., 2017, Bretherton et al., 2005, Emanuel et al., 2014, Gill, 1980, Wing & Emanuel, 2013). Perhaps the most significant simplifying assumption of the model is to neglect these other important processes and represent tropical circulations as a function of SST gradients alone.

With these parameterizations the clouds, ocean, and atmosphere regulate one another through a negative feedback process. For instance, if a warm SST anomaly develops in the convective region, then it increases the SST gradient and strengthens the overturning cell. This increases upward motion and albedo in the convective region, which dampens the warm SST anomaly. If the feedback is sufficiently strong, then even a small SST gradient drives a strong circulation response, so SST gradients are constrained to be small. Small SST gradients reduce the horizontal energy transport by the overturning cell, and if horizontal energy transport is sufficiently reduced, then the top-of-atmosphere net radiation must be similar in the convective and nonconvective regions to close the energy budget. Thus, the feedback drives the net CRE in the convective region toward that in the nonconvective region.

The relationship between spatial variations in net radiation and spatial variations in net CRE also depends on the radiative effects of water vapor, however, because convective regions systematically contain more water vapor than nonconvective regions. If spatial variations in water vapor do not substantially modify spatial variations in clear-sky radiative fluxes, then uniform net radiation implies near-uniform net CRE. Indeed, spatial variations in column water vapor within the warm pool region rarely exceed 10% of the large-scale average column water vapor (Lebsock et al., 2017). For humidity profiles typical of the warm pool, a 10% increase in free tropospheric relative humidity reduces clear-sky outgoing LW radiation by about 5 W/m^2 (Roca et al., 2012; Tobin et al., 2012). Spatial variations in humidity therefore have a modest influence on spatial variations in clear-sky radiative fluxes over spatial scales comparable to the size of the warm pool. Thus, the Hartmann et al. (2001) model predicts that net radiation and net CRE will be nearly uniform over the warm pool if the feedback process is sufficiently strong.

The Hartmann et al. (2001) model is meant to represent the interactions among cloud albedo, SST, and atmospheric circulation, which we will henceforth call the “cloud shading feedback.” By modeling this feedback in isolation, however, many other processes that link atmospheric moisture and circulation are simplified or neglected. A key goal of this study is to test if the behavior of the Hartmann et al. (2001) model is seen in a more realistic model that includes other processes.

3. Methods

We run the Community Atmosphere Model version 4 (CAM4), which is a global atmosphere model (Neale et al., 2011). A grid spacing of 1.9° latitude, 2.5° longitude, and 27 vertical levels is used. All simulations are run for 5 years, after spinning up the model for 2 years, and daily output is analyzed.

The model is run in the simplest configuration that explicitly represents the cloud shading feedback. For the atmospheric component of the model, we use a global radiative-convective equilibrium configuration following the standard procedure of the radiative-convective equilibrium model intercomparison project (Wing et al., 2018): (1) The planet is entirely ocean covered and is not rotating; (2) atmospheric CO_2 concentration is set to 348 ppmv; (3) surface albedo is set to 0.07; (4) the solar constant and solar zenith angle are set to 551.58 W/m^2 and 42.05° , respectively, which reproduce the annual mean insolation in the tropics; and (5) aerosol effects are excluded. The atmosphere model is coupled with a thermodynamic ocean model using

a mixed-layer depth of 5 m, which is typical of oceanic diurnal warm layers observed in the tropical western Pacific (Soloviev & Lukas, 1996; Soloviev & Lukas, 2006). We follow the recommendation of the radiative-convective equilibrium model intercomparison project and apply a uniform heat sink to the ocean mixed layer to prevent the mean SST from becoming unrealistically warm. Our “Control” simulation with the aforementioned settings equilibrates to a long-term mean SST of 26 °C. The results are not sensitive to changing the mixed-layer depth to 30 m or varying the long-term mean SST between 29 and 21 °C by changing the heat sink that is applied to the ocean mixed layer (Figures S8 and S9).

One may ask if such a model is useful for testing the hypothesis, given that it parameterizes cloud physics and convection. Despite this limitation, the model conserves energy and resolves motions around 1,500 km in scale, which are relevant to the hypothesis. Furthermore, the reduction of surface insolation beneath convective clouds, which is a key element of the cloud shading feedback, should be captured even with simple cloud parameterizations. Indeed, we verified that the model simulates the cloud shading feedback and that the amplitude and timescale of the SST fluctuations agree with observations (Wall et al., 2018; Figure S3).

We use two experiments to investigate the hypothesis. First, the “Control” experiment is run, in which clouds, SST, and atmospheric circulation interact naturally with one another. The SW fluxes at the ocean surface are saved at every time step of the Control simulation for later use. These fluxes are then randomly permuted in the time dimension, and a “Random SW” experiment is performed in which the simulated SW fluxes at the ocean surface are overwritten by the randomized fluxes from the Control simulation. At each grid point at the ocean surface, the distribution of SW flux is identical in the two simulations, but the time sequence in which the values occur is different. In the Control simulation, a warm SST anomaly can generate upward motion and convective clouds that shade the surface and feed back on the SST. This cannot happen in the Random SW simulation, however, because whatever SW heating of the ocean that might occur is unrelated to the atmospheric circulation and SST anomaly at that time. Comparing the two simulations allows us to understand the relevance of the cloud shading feedback for tropical climate and to test the hypothesis of Hartmann et al. (2001).

We also perform additional simulations to check the results and to aid in the interpretation. A “Uniform SST” simulation is performed in which SST is fixed to a uniform, constant value equal to the long-term global-mean SST from the Control simulation. The Uniform SST simulation represents the limiting case in which SST gradients are completely removed, so it is a useful benchmark to compare with the Control simulation. We also perform a “Uniform SW” simulation that is similar to the Uniform SST case except that surface SW heating is held constant instead of SST. The Uniform SW and Random SW simulations are compared to check if the results are sensitive to the method of removing the cloud shading feedback, whether it be randomizing or fixing surface SW heating. The Uniform SW and Random SW simulations have very similar climates, so the results are not sensitive to the method of removing the cloud shading feedback (Figures S5 and S6). Finally, we run simulations that are similar to the Control case but have perturbed atmospheric CO₂ concentration and solar constant. CO₂ concentrations are varied from 0.25 times the Control value and successively doubled up to 8 times the Control value, and the solar constant is varied from 0.98 to 1.02 times the Control value in increments of 0.01. These simulations are used to check if certain features of the Control simulation are sensitive to changes in climate. The mean SST from these simulations is listed in Table S1.

4. Results

4.1. Hypothesis Testing

The hypothesis in question predicts that the cloud shading feedback reduces SST gradients, which reduces the lateral energy transport by the atmosphere, which reduces the net CRE contrast between convective and nonconvective regions over the warm pool. If this hypothesis is correct, then relative to the Control climate, the Random SW climate will have significantly larger SST gradients, larger atmospheric energy transport, and larger net CRE contrast between convective and nonconvective regions. Alternatively, if the hypothesis is incorrect and the cloud shading feedback is unimportant for the radiation budget, then the Control and Random SW simulations will have similar climates because the overall surface SW heating is identical in the two simulations. We will now compare the two simulations, keeping these potential outcomes in mind.

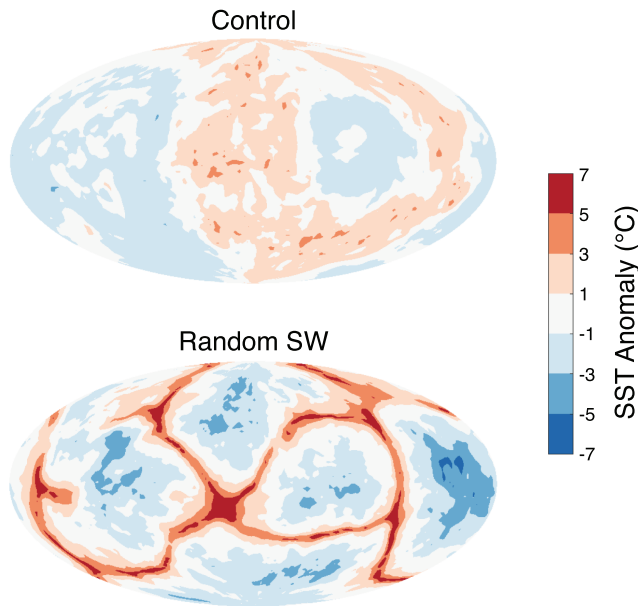


Figure 2. Snapshots showing typical sea surface temperature (SST) patterns. SST anomalies relative to the global mean are shown. The long-term global-mean SST is 26 °C in the Control case and 19 °C in the Random shortwave (SW) case.

We begin by considering snapshots from the simulations, which are shown in Figure 2. These display features of the global SST patterns that are typical of the two simulations. The Control climate has broad warm and cold pools, the largest of which are the size of Earth's ocean basins. In the Random SW case, however, the warm pools have larger warm anomalies, are arranged in narrow bands, and are flanked by much larger SST gradients. These differences arise because different processes regulate SST in the two simulations. In the Control case, the dominant process regulating SST is cloud shading and secondarily evaporative cooling, but in the Random SW case, the dominant process is evaporative cooling and secondarily LW cooling (Figure S4). The processes in the Random SW case are less efficient in removing warm SST anomalies and allow larger SST gradients to develop. These SST gradients, in turn, strengthen the atmospheric circulation and modify other aspects of climate. For instance, the global-mean near-surface wind speed is 53% larger in the Random SW case. This increases the efficiency of surface evaporative cooling in the subsidence regions, which cools the long-term global-mean SST from 26 °C in the Control case to 19 °C in the Random SW case (Table S2; Hartmann & Michelsen, 1993). Convection also strongly aggregates over the warm bands in the Random SW simulation, suggesting that the cloud shading feedback substantially limits the degree of large-scale convective aggregation in the tropics (see also Coppin & Bony, 2018).

Statistics of SST anomalies are shown in Figures 3a and 3b. The SST anomalies are computed by removing the global-mean SST from each simulation day so as to emphasize horizontal variations in SST. The distribution of SST anomalies is partitioned into contributions from grid points with net ascent and grid points with net subsidence in the troposphere. The Control simulation, in which the cloud shading feedback is active, exhibits an SST contrast between ascending and subsiding regions that is around 1 °C, whereas the Random SW simulation, in which the cloud shading feedback is not active, exhibits a larger SST contrast that is around 4 °C. The cloud shading feedback therefore significantly reduces tropical SST gradients.

We are now ready to investigate the second element of the hypothesis, which is that small SST gradients reduce the efficiency of lateral energy transport by the atmospheric circulation. We investigate this using the column moist static energy budget. The column moist static energy, H , is defined as

$$H \equiv \int_{p_t}^{p_s} (c_p T + Lq + gz) \frac{dp}{g},$$

where c_p is the specific heat capacity of dry air, T is temperature, L is the latent heat of vaporization, q is specific humidity, g is acceleration due to gravity, z is geopotential height, p_s is surface pressure, and $p_t = 50$ hPa is above the tropopause. We neglect the contribution of ice to moist static energy because it is much smaller than the other terms in the above equation. The tendency of H is equal to the sum of the sources and sinks of energy:

$$\frac{\partial H}{\partial t} = S + R_{\text{atm}} - D,$$

where S is the surface flux of latent and sensible heat, R_{atm} is the column-integrated radiative heating of the atmosphere, and D is the column-integrated energy flux divergence due to the atmospheric circulation. We compute D as a residual of the above equation, and for each simulation day, we average it over the grid points with net upward motion in the troposphere. This quantity represents the energy exported from ascending regions by the atmospheric circulation.

The energy exported from ascending regions is shown in Figure 3c. Energy transport in the Uniform SST simulation represents that which the atmosphere can achieve in the absence of SST gradients but with the same long-term mean SST as the Control case. The average energy exported from ascending regions is

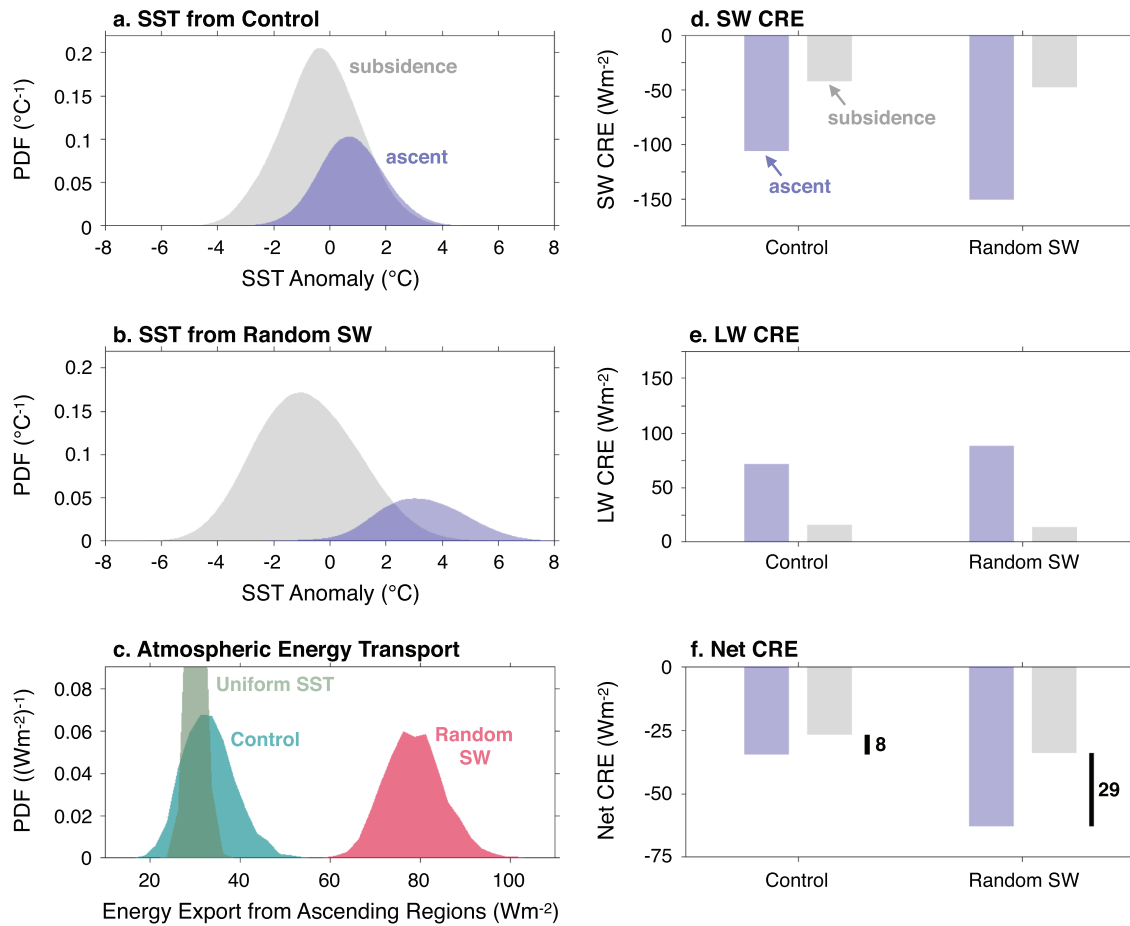


Figure 3. Statistics of sea surface temperature (SST) gradients, lateral atmospheric energy transport, and cloud radiative effect (CRE). (a) Area-weighted probability density function (PDF) of SST anomalies from the Control simulation. SST anomalies are computed by removing the global-mean SST from each simulation day so as to emphasize horizontal variations in SST. The PDFs are decomposed into contributions from the grid points with net ascent and grid points with net subsidence in the troposphere. (b) Similar to (a) but for the Random shortwave (SW) simulation. (c) The energy exported from ascending regions by the atmospheric circulation. Each point in the histogram represents the average energy export from ascending regions during one simulation day. PDFs are shown for the Uniform SST, Control, and Random SW simulations. (d) The average SW CRE in ascending regions and in subsiding regions for the Control and Random SW simulations. (e, f) Similar to (d) but for longwave (LW) CRE and net CRE, respectively. Note the scale difference between (d, e) and (f). The black lines and numbers in (f) show the net CRE contrast between ascending and subsiding regions.

30 W/m² in the Uniform SST case, in which SST gradients do not occur, and 35 W/m² in the Control case, in which SST gradients do occur but are constrained to be small by the cloud shading feedback. The distribution of energy transport is wider in the Control case than in the Uniform SST case because the inclusion of an interactive ocean permits natural variability in the global-mean SST and SST gradients, which both influence atmospheric energy transport (Figure S2; Coppin & Bony, 2017). In contrast to the Control and Uniform SST simulations, the average energy transport in the Random SW simulation is 79 W/m², which is much larger. Energy transport is similar in the Random SW and Uniform SW simulations (Figure S6). The cloud shading feedback therefore reduces lateral atmospheric energy transport by slightly more than a factor of 2 and constrains the energy transport to be close to what the atmosphere would achieve in the absence of SST gradients.

Now we can investigate the final element of the hypothesis, which is that reduced atmospheric energy transport is associated with more uniform net CRE. The components of CRE averaged over ascending and subsiding regions are shown in Figures 3d–3f. In the Control simulation the net CRE is more negative than observed values over the tropical warm pools (Figure 1). However, the net CRE contrast between ascending and subsiding regions is 8 W/m², which is an order of magnitude smaller than the SW CRE and LW CRE in

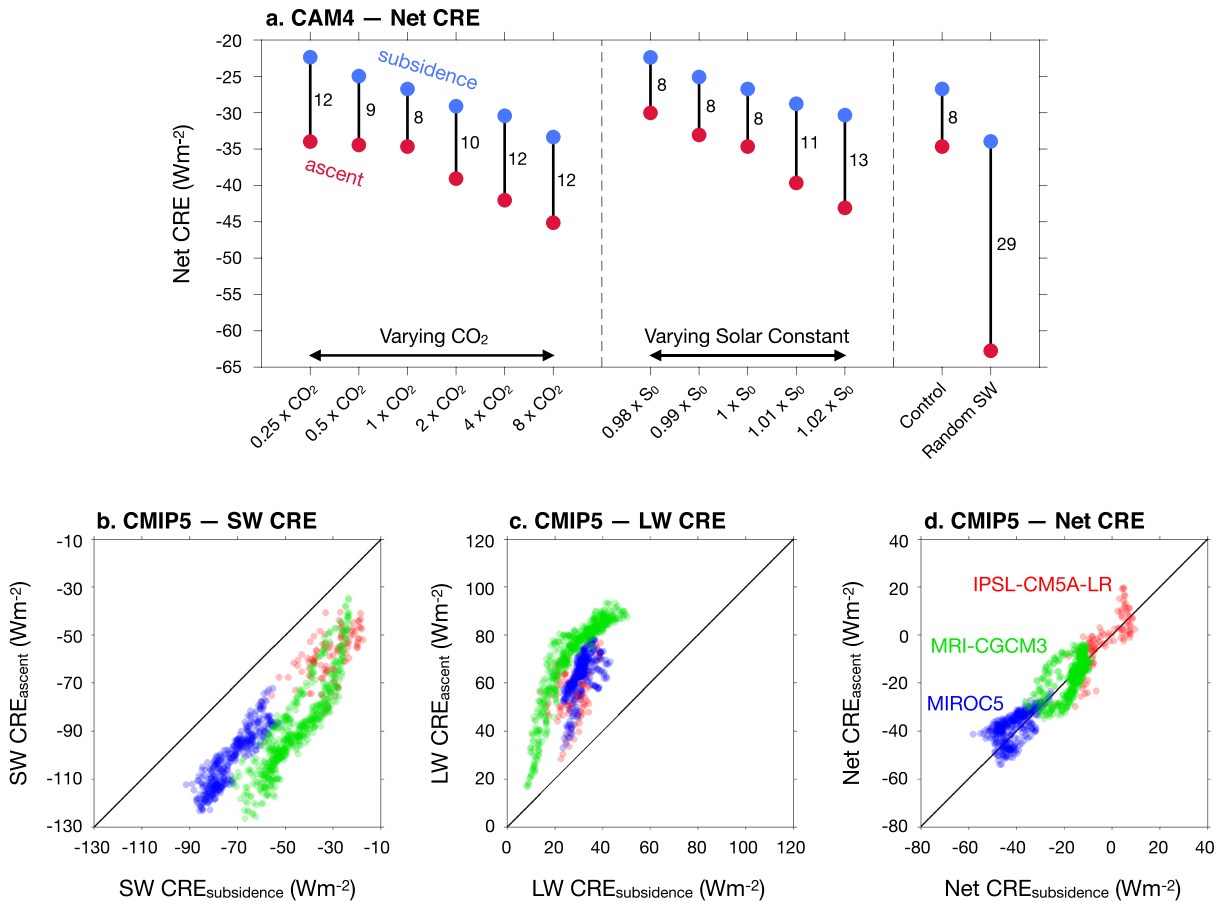


Figure 4. Average cloud radiative effect (CRE) for ascending and subsiding conditions in Community Atmosphere Model version 4 (CAM4) and three fully coupled Model Intercomparison Project Phase 5 (CMIP5) models. (a) Net CRE averaged over ascending and subsiding regions from CAM4 simulations with varying atmospheric CO₂ concentration and solar constant, as indicated on the horizontal axis. Numbers on the figure show the net CRE contrast between ascending and subsiding regions. The Control and Random shortwave (SW) simulations are shown on the right. (b) SW CRE_{ascent} plotted as a function of SW CRE_{subsidence} from historical simulations of three fully coupled CMIP5 models. Data from the west Pacific warm pool region are plotted. Each point in the scatterplot represents a single grid cell, and each color represents a different model. The diagonal shows the one-to-one line. (c, d) Similar to (b) but showing longwave (LW) CRE and net CRE, respectively. Model names are indicated in (d).

ascending regions. The climate of the Control simulation is therefore consistent with the hypothesis even though the average net CRE is biased. Meanwhile, the Random SW simulation exhibits a substantially larger net CRE contrast between ascending and subsiding regions that is around 29 W/m². The enhanced net CRE contrast in the Random SW simulation results mostly from a brightening of the convective clouds, which is likely due to the circulation shifting toward deeper overturning motion and stronger updrafts (Figure S7). Note that the cloud shading feedback also reduces the degree of aggregation of the convection, increasing the area of upward motion from 20% of the domain in the Random SW case to 30% in the Control case (see also Coppin & Bony, 2018; Figure S9).

These findings support the hypothesis of Hartmann et al. (2001). They show that, in an idealized model setup, the cloud shading feedback reduces the net CRE contrast between ascending and subsiding regions over the tropical oceans.

4.2. A Note on Model Tuning

We have shown that in the Control case the net CRE contrast between ascending and subsiding regions is an order of magnitude smaller than the SW CRE and LW CRE in ascending regions, which is consistent with the hypothesis that the cloud shading feedback dampens inhomogeneities in net CRE. But could this feature occur simply because the tuning parameters of the model were chosen to produce it? To investigate this possibility we examine simulations that are similar to the Control case except that the atmospheric CO₂

concentration and solar constant are varied. Figure 4a shows net CRE from these simulations. The net CRE contrast between ascending and subsiding regions varies between 8 and 13 W/m² and is much smaller than the net CRE contrast in the Random SW case. Since model tuning is performed at modern conditions, it cannot explain why the net CRE contrast remains small and nearly constant as substantial radiative forcing is applied. The cloud shading hypothesis is consistent with this result, however, because the mechanism is active in the perturbed climates.

We also investigate the sensitivity of the results to model tuning by examining output from other models. We consider historical simulations from IPSL-CM5A-LR, MIROC5, and MRI-CGCM3, which are fully coupled models from the Coupled Model Intercomparison Project Phase 5 (CMIP5). Daily output is analyzed from June–August of 1979–2005 and from the west Pacific warm pool region, which we define as 15°S to 15°N and 140–170°E. Remote ocean locations that are at least 500 km from the nearest land-covered grid cell are selected for analysis, and CRE is averaged over the days with ascending motion and over the days with subsiding motion at 500 hPa. We call these quantities CRE_{ascent} and CRE_{subsidence}, respectively.

Figure 4b shows SW CRE_{ascent} and SW CRE_{subsidence} for all locations in the warm pool in the three models. All points lie below the diagonal because convective clouds, which occur on days of ascent, are brighter than boundary-layer clouds, which occur on days of subsidence. Differences in SW CRE_{ascent} between models are tens of watts per square meter, as are those of SW CRE_{subsidence}, LW CRE_{ascent}, and LW CRE_{subsidence} (Figures 4b and 4c). This suggests that the models have substantial differences in their cloud parameterizations and tuning. Despite these differences in SW CRE and LW CRE, all three models have a small net CRE contrast between ascending and subsiding conditions (Figure 4d). In fact, net CRE_{ascent} is within 10 W/m² of net CRE_{subsidence} for around 90% of the warm pool region in all three models. Tuning cannot be the explanation for this feature because the overall net CRE differs by tens of watts per square meter between the models. The cloud shading hypothesis is consistent with this result, however, because it applies to all three models.

5. Conclusion

A long-standing open problem in climate research is to explain why the net CRE is about the same in convective and nearby nonconvective regions over the tropical warm pools, despite the fact that the average SW CRE and LW CRE of deep convective clouds are both large. One hypothesis suggests that the shading effect of convective clouds on the underlying ocean maintains small SST gradients and reduces lateral atmospheric energy transport within the warm pool region. If atmospheric energy transport is sufficiently reduced, then net CRE is constrained to be similar in convective and nearby nonconvective regions to close the energy budget (Hartmann et al., 2001). We have investigated this hypothesis using an idealized model of the tropical ocean-atmosphere system. Preventing cloud shading effects from mutually interacting with the SST and atmospheric circulation results in large enhancements in SST gradients, atmospheric energy transport, convective aggregation, and the net CRE of convective clouds. These findings support the hypothesis and indicate that the cloud shading interaction is critical to obtaining uniform net CRE across the convective and nonconvective regions of the warm pools.

For future research, a relevant goal is to determine if the cloud shading interaction is sufficient to guarantee the degree of uniformity of net CRE that is observed or if some additional logic is needed. In our simulations the cloud shading interaction substantially reduces lateral atmospheric heat transport but does not cause it to vanish, so we do not reach a conclusion about sufficiency of the theory. Testing for sufficiency is important, however, because it would indicate if the cloud shading interaction will influence the cloud response to anthropogenic radiative forcing. For instance, if the cloud shading interaction acts to maintain similar net CRE in convective and nonconvective regions in the future, as our simulations suggest could happen (Figure 4a), then this would imply that the response of deep convective clouds to anthropogenic forcing is linked to the response of trade cumulus. Future studies should therefore consider the implications of the cloud shading interaction for tropical cloud-climate feedbacks.

References

- Back, L. E., & Bretherton, C. S. (2009). On the relationship between SST gradients, boundary layer winds, and convergence over the tropical oceans. *Journal of Climate*, 22(15), 4182–4196. <http://doi.org/10.1175/2009JCLI2392.1>
- Becker, T., Stevens, B., & Hohenegger, C. (2017). Imprint of the convective parameterization and sea-surface temperature on large-scale convective self-aggregation. *Journal of Advances in Modeling Earth Systems*, 9, 1488–1505. <https://doi.org/10.1002/2016MS000865>

Acknowledgments

This research is supported by the NOAA Climate and Global Change Postdoctoral Fellowship Program, administered by UCAR's Cooperative Programs for the Advancement of Earth System Science (CPAESS) under award NA18NWS4620043B. C. J. W. and D. L. H. were also supported by NASA Grant NNX14AJ26G to the University of Washington. We gratefully acknowledge Paulo Ceppi, Cecilia Bitz, Brian Medeiros, and Kevin Reed for sharing code that was helpful for setting up the model simulations; Frida Bender, Chris Bretherton, and Mark Zelinka for insightful discussions that improved this study; and Thorsten Mauritsen and an anonymous reviewer for helpful comments. The CAM4 output is available at ftp://eos.atmos.washington.edu/pub/caseyw8/tropic_world, the CMIP5 output is available at <https://esgf-node.llnl.gov/projects/cmip5/>, and the CERES data are available at <https://ceres.larc.nasa.gov/>.

- Bretherton, C. S., Blossey, P. N., & Khairoutdinov, M. (2005). An energy-balance analysis of deep convective self-aggregation above uniform SST. *Journal of the Atmospheric Sciences*, *62*(12), 4273–4292. <http://doi.org/10.1175/JAS3614.1>
- Clement, A. C., & Seager, R. (1999). Climate and the tropical oceans. *Journal of Climate*, *12*(12), 3383–3401. [http://doi.org/10.1175/1520-0442\(1999\)012<3383:CATTO>2.0.CO;2](http://doi.org/10.1175/1520-0442(1999)012<3383:CATTO>2.0.CO;2)
- Coppin, D., & Bony, S. (2017). Internal variability in a coupled general circulation model in radiative-convective equilibrium. *Geophysical Research Letters*, *44*, 5142–5149. <https://doi.org/10.1002/2017GL073658>
- Coppin, D., & Bony, S. (2018). On the interplay between convective aggregation, surface temperature gradients, and climate sensitivity. *Journal of Advances in Modeling Earth Systems*, *10*(12), 3123–3138. <http://doi.org/10.1029/2018MS001406>
- Emanuel, K., Wing, A. A., & Vincent, E. M. (2014). Radiative-convective instability. *Journal of Advances in Modeling Earth Systems*, *6*, 75–90. <http://doi.org/10.1002/2013MS000270>
- Gasparini, B., Blossey, P. N., Hartmann, D. L., Lin, G., & Fan, J. (2019). What drives the lifecycle of tropical anvil clouds? *Journal of Advances in Modeling Earth Systems*, *11*(8), 2586–2605. <https://doi.org/10.1029/2019MS001736>
- Gill, A. E. (1980). Some simple solutions for heat induced tropical circulation. *Quarterly Journal of the Royal Meteorological Society*, *106*(449), 447–462. <http://doi.org/10.1002/qj.49710644905>
- Hartmann, D. L., & Berry, S. E. (2017). The balanced radiative effect of tropical anvil clouds. *Journal of Geophysical Research: Atmospheres*, *122*, 5003–5020. <http://doi.org/10.1002/2017JD026460>
- Hartmann, D. L., & Michelsen, M. L. (1993). Large scale effects on the regulation of tropical sea surface temperature. *Journal of Climate*, *6*(11), 2049–2062. [https://doi.org/10.1175/1520-0442\(1993\)006<2049:LSEOTR>2.0.CO;2](https://doi.org/10.1175/1520-0442(1993)006<2049:LSEOTR>2.0.CO;2)
- Hartmann, D. L., Moy, L. A., & Fu, Q. (2001). Tropical convection and the energy balance at the top of the atmosphere. *Journal of Climate*, *14*(24), 4495–4511. [http://doi.org/10.1175/1520-0442\(2001\)014<4495:TCATEB>2.0.CO;2](http://doi.org/10.1175/1520-0442(2001)014<4495:TCATEB>2.0.CO;2)
- Lebsock, M. D., L'Ecuyer, T. S., & Pincus, R. (2017). An observational view of relationships between moisture aggregation, cloud, and radiative heating profiles. *Surveys in Geophysics*, *38*(6), 1237–1254. <http://doi.org/10.1007/s10712-017-9443-1>
- Li, R. L., Storelvmo, T., Fedorov, A. V., & Choi, Y. (2019). A positive iris feedback: Insights from climate simulations with temperature-sensitive cloud–rain conversion. *Journal of Climate*, *32*, 5305–5324. <https://doi.org/10.1175/JCLI-D-18-0845.1>
- Li, Y., & Carbone, R. E. (2012). Excitation of rainfall over the tropical western Pacific. *Journal of the Atmospheric Sciences*, *69*(10), 2983–2994. <http://doi.org/10.1175/jas-d-11-0245.1>
- Lindzen, R. S., & Nigam, S. (1987). On the role of sea surface temperature gradients in forcing low-level winds and convergence in the tropics. *Journal of the Atmospheric Sciences*, *44*(17), 2418–2436. [https://doi.org/10.1175/1520-0469\(1987\)044<2418:OTROSS>2.0.CO;2](https://doi.org/10.1175/1520-0469(1987)044<2418:OTROSS>2.0.CO;2)
- Miller, R. L. (1997). Tropical thermostats and low cloud cover. *Journal of Climate*, *10*(3), 409–440. [http://doi.org/10.1175/1520-0442\(1997\)010<0409:TTALCC>2.0.CO;2](http://doi.org/10.1175/1520-0442(1997)010<0409:TTALCC>2.0.CO;2)
- Neale, R. B., Jadwiga H. Richter, Andrew J. Conley, Sungsu Par, Peter H. Lauritzen, Andrew Gettelman, et al., (2011). Description of the NCAR Community Atmosphere Model (CAM4). NCAR Tech. Note NCAR/TN-4851STR, 120 pp.
- Peters, M. E., & Bretherton, C. S. (2005). A simplified model of the Walker circulation with an interactive ocean mixed layer and cloud-radiative feedbacks. *Journal of Climate*, *18*(20), 4216–4234. <http://doi.org/10.1175/JCLI3534.1>
- Pierrehumbert, R. T. (1995). Thermostats, radiator fins, and the local runaway greenhouse. *Journal of the Atmospheric Sciences*, *52*(10), 1784–1806. [https://doi.org/10.1175/1520-0469\(1995\)052<1784:TRFATL>2.0.CO;2](https://doi.org/10.1175/1520-0469(1995)052<1784:TRFATL>2.0.CO;2)
- Roca, R., Guzman, R., Lemond, J., Meijer, J., Picon, L., & Brogniez, H. (2012). Tropical and extra-tropical influences on the distribution of free tropospheric humidity over the intertropical belt. *Surveys in Geophysics*, *33*(3–4), 565–583. <http://doi.org/10.1007/s10712-011-9169-4>
- Soloviev, A., & Lukas, R. (1996). Observation of spatial variability of diurnal thermocline and rain-formed halocline in the western Pacific warm pool. *Journal of Physical Oceanography*, *26*(11), 2529–2538. [http://doi.org/10.1175/1520-0485\(1996\)026<2529:OOSVOD>2.0.CO;2](http://doi.org/10.1175/1520-0485(1996)026<2529:OOSVOD>2.0.CO;2)
- Soloviev, A., & Lukas, R. (2006). *The near-surface layer of the ocean*, (p. 572). Netherlands: Springer.
- Tobin, I., Bony, S., & Roca, R. (2012). Observational evidence for relationships between the degree of aggregation of deep convection, water vapor, surface fluxes, and radiation. *Journal of Climate*, *25*(20), 6885–6904. <http://doi.org/10.1175/JCLI-D-11-00258.1>
- Wall, C. J., & Hartmann, D. L. (2018). Balanced cloud radiative effects across a range of dynamical conditions over the tropical west Pacific. *Geophysical Research Letters*, *5*, 1–9. <http://doi.org/10.1029/2018GL080046>
- Wall, C. J., Hartmann, D. L., Thieman, M. M., Smith, W. L., & Minnis, P. (2018). The life cycle of anvil clouds and the top-of-atmosphere radiation balance over the tropical west Pacific. *Journal of Climate*, *31*(24), 10,059–10,080. <http://doi.org/10.1175/JCLI-D-18-0154.1>
- Wing, A. A., & Emanuel, K. A. (2013). Physical mechanisms controlling self-aggregation of convection in idealized numerical modeling simulations. *Journal of Advances in Modeling Earth Systems*, *59*–74. <http://doi.org/10.1002/2013MS000269>. Received
- Wing, A. A., Reed, K. A., Satoh, M., Stevens, B., Bony, S., & Ohno, T. (2018). Radiative-convective equilibrium model intercomparison project. *Geoscientific Model Development*, *11*(2), 793–813. <http://doi.org/10.5194/gmd-11-793-2018>